ASYMPTOTIC SOLUTION FOR THE ORBIT MOTION UNDER CONSTANT TANGENTIAL ACCELERATION[1]

Claudio Bombardelli(1), **Giulio Baú** (2), **Jesús Peláez**(1)

(1) *Universidad Politécnica de Madrid, 28040 Madrid, Spain, +34 913 366 306, claudio.bombardelli@upm.es,*

(2) *University of Padova, CISAS "G. Colombo", via Venezia 15, 35131 Padova, Italy, +39 049 82768485, giulio.bau@unipd.it*

Abstract: *We present an analytical method for propagating the orbital motion of a spacecraft perturbed by a constant tangential acceleration. The solution is obtained starting from the orbital element formulation recently proposed by Pelaez et al. and applying perturbation theory. Analytical expressions valid for elliptic orbits with generic eccentricity, describe the instantaneous time variation of all orbital elements. A comparison with high-accuracy numerical results is carried out showing that the analytical method can be effectively applied to multiple-revolution low-thrust orbit transfer around planets and in interplanetary space. The limits of the applicability of the method, which depend on the the ratio between the tangential ecceleration and the local gravity, are discussed.*

Keywords: *Low thrust, Orbital Dynamics, Perturbation Theory*

1 Introduction

The study of the orbit evolution of a spacecraft under the perturbation of a constant tangential acceleration has important implications in orbital dynamics. It is well known, for instance, that a purely tangential thrust provides a maximum *instantaneous* rate of orbital energy increase and can be useful in the process of finding optimal solutions for the maximization of such energy along a generic time span[2]. In addition, as high-specific-impulse propulsion systems provide a relatively small thrust primarily due to the cost, in terms of hardware mass, of the required onboard power, the tangential thrust magnitude is typically small compared with local gravity and is applied contnuously over a time period that is at least of the same order of the period of the osculating orbit or even orders of magnitude larger.

For these reasons many authors have proposed analytical or semianalytical solutions for the propagation of orbits under constant or variable tangential

[1] An extended version of this article was submitted to the journal of Celestial Mechanics and Dynamical Astronomy.

[2] The maximum increase in the orbital energy over a fixed period of time or, equivalently, the minimum time for a specific energy increase is obtained when the thrust is aligned with the primer vector minimizing the Hamiltonian associated with the optimum control problem.

acceleration ([1],[2], [3], [4],[5]). These methods, which can be effective in reproducing the secular variations of slowly spiralling circular and even elliptical orbits, cannot in general reproduce oscillatory variations of the orbital elements and lose accuracy when the ratio beteen the thrust magnitude and local gravity increases beyond say 1×10^{-3}. For these reasons they may show degraded performance when applied to the propagation of interplanetary trajectories when realistic level of achievable accelerations can make a trajectory consideably far from keplerian.

In order to overcome this limitation we have developed an approximate, yet accurate analytical model[6] to represent the average *and* oscillatory time evolution of all orbital elements by exploiting the use of perturbation theory and of a non-singular variation of parameter formulation of the orbital dyanmics[7].

Assuming the acceleration magnitude is small (say $\epsilon < 0.1$) when compared to the local gravity we formulate the orbit dynamics problem as a general perturbation problem. After a straightforward series expansion the first-order time evolution of the three generalized orbital elements associated to the planar orbital motion are obtained, in analytical close form, by simple quadrature. Secular and oscillatory terms are both computed, which are generally a combination of elliptic integrals of the first and second kind. Trigonometric series for the oscillatory terms are given in order to speed up the computation process and allow the computation of second-order terms. The effectiveness of the approximate analytical solution is tested for a transfer from GTO to Earth escape and from Earth to Mercury, in both cases assuming continuous and constant tangential acceleration and no orbit plane change.

2 Equations of Motion

Let us consider a particle orbiting around a primary at initial radial position r_0 measured from the center of the primary and angular position θ_0 measured from the initial eccentricity vector. Let us employ, from now on, r_0 as unit of distance and $1/\Omega_0$ as unit of time where Ω_0 is the angular rate of a circular orbit with radius equal to the initial radius r_0:

$$\Omega_0 = \sqrt{\frac{\mu}{r_0^3}},$$

with μ indicating the gravitational parameter of the primary.

Using the formulation described by Pelaez et al. ([7]), and under the hypothesis that all acting perturbation forces have zero component along the normal to the orbital plane, the orbit geometry can be fully described by the three generalized orbital parameters:

$$q_1 = \frac{e}{h} \cos \Delta\gamma, \tag{1}$$

$$q_2 = \frac{e}{h} \sin \Delta\gamma, \tag{2}$$

$$q_3 = \frac{1}{h}, \tag{3}$$

where h is the dimensionless angular momentum of the osculating orbit, e its eccentricity and $\Delta\gamma$ is, for the constant orbit plane case, the rotation of the eccentricity vector with respect to the initial orbit.

From the above expressions the orbit eccentricity, the eccentricity vector rotation and the non-dimensional angular momentum can be written, for later use as:

$$e = \frac{\sqrt{q_1^2 + q_2^2}}{q_3}, \tag{4}$$

$$\Delta\gamma = \tan^{-1}\left(\frac{q_2}{q_1}\right), \tag{5}$$

$$h = \frac{1}{q_3}. \tag{6}$$

The expression of the non-dimensional semimajor axis is then:

$$a = \frac{h^2}{1 - e^2} = \frac{1}{q_3^2 - q_1^2 - q_2^2}. \tag{7}$$

The independent variable used in the Pelaez method is, again for the planar case ([7]):

$$\theta = \nu + \Delta\gamma, \tag{8}$$

where ν is the true anomaly of the osculating orbit. Note that θ corresponds to the inertial angular position of the particle measured from the initial eccentricity vector.

A Sundmann transformation, corresponding the the angular momentum variation equation, relates θ to the dimensionless time t as:

$$\frac{d\theta}{dt} = \frac{h}{r^2} = q_3 s^2, \tag{9}$$

where s is the dimensionless transverse velocity of the particle and obeys ([7]):

$$s = q_1 \cos\theta + q_2 \sin\theta + q_3. \tag{10}$$

The orbit radius as a function of the generalized orbital parameter can be obtained from the two equations above as:

$$r(\theta) = (q_3 s)^{-1} = \left(q_3^2 + q_1 q_3 \cos\theta + q_2 q_3 \sin\theta\right)^{-1}. \tag{11}$$

The evolution of the three generalized orbital parameters obeys (see[7]):

$$\frac{d}{d\theta}\begin{pmatrix} q_1 \\ q_2 \\ q_3 \end{pmatrix} = \frac{1}{q_3 s^3}\begin{pmatrix} s\,\sin\theta & (s+q_3)\cos\theta \\ -s\,\cos\theta & (s+q_3)\sin\theta \\ 0 & -q_3 \end{pmatrix}\begin{pmatrix} a_r \\ a_\theta \end{pmatrix}, \tag{12}$$

where a_r and a_θ are, respectively, the component of the dimensionless perturbative acceleration along the instantaneous radial and transversal direction.

If the acceleration is always directed along the instantaneous velocity vector Eq.s (12) become:

$$\frac{d}{d\theta}\begin{pmatrix} q_1 \\ q_2 \\ q_3 \end{pmatrix} = \frac{\epsilon}{q_3 s^3\sqrt{e^2+2e\cos\nu+1}}\begin{pmatrix} s\,\sin\theta & (s+q_3)\cos\theta \\ -s\,\cos\theta & (s+q_3)\sin\theta \\ 0 & -q_3 \end{pmatrix}\begin{pmatrix} e\sin\nu \\ 1+e\cos\nu \end{pmatrix}, \tag{13}$$

where $\epsilon = \sqrt{a_r^2+a_\theta^2}$ is the dimensionless tangential acceleration magnitude. Note that, by use of Eq.s(4,5,8,10), the above equations can be put in the form:

$$\frac{d\boldsymbol{q}}{d\theta} = \boldsymbol{F}(\boldsymbol{q},\epsilon,\theta), \tag{14}$$

where $\boldsymbol{q} = (q_1,q_2,q_3)^T$ and $\boldsymbol{F}$ is a nonlinear vectorial function.

Equations (14) must be integrated with the appropriate initial conditions namely:

$$q_1(\theta_0) = e_0/h_0,$$

$$q_2(\theta_0) = 0,$$

$$q_3(\theta_0) = 1/h_0.$$

3 Asymptotic Solution

When considering high specific impulse electric propulsion systems, currently the most common low-thrust solution employed in space technology, typical values for the achievable acceleration with resonable payload masses range around 100 mN/tonne [8]. In most circumstances (depending on the local gravity value for the particular orbit considered) the resulting dimensionless acceleration ϵ will also be a small quantity which will be used to perform an asymptotic expansion of Eqs. (13) and (9), which characterize, respectively, the trajectory geometry and its evolution in time.

3.1 Trajectory

In the hypothesis that ϵ is a small quantity we write the three generalized orbital elements as power series:

$$q_i(\theta,\epsilon) = q_{i0}(\theta) + \epsilon q_{i1}(\theta) + \epsilon^2 q_{i2}(\theta) + o(\epsilon^2) \quad i = 1..3. \tag{15}$$

Substituting into Eq.s (14) , expanding in Taylor series and solving for like powers of epsilon we obtain, for the zeroth order:

$$\frac{dq_{i0}}{d\theta} = 0,$$

showing that the zeroth order terms are just the (constant) generalized orbital elements of the unperturbed trajectory:

$$q_{10} = e_0/h_0, \tag{16}$$

$$q_{20} = 0, \tag{17}$$

$$q_{30} = 1/h_0, \tag{18}$$

where e_0 and h_0 are, respectively, the eccentricity and dimensionless angular momentum of the initial trajectory.

The differential equations for the first order terms results:

$$\frac{d}{d\theta}\begin{pmatrix} q_{11} \\ q_{21} \\ q_{31} \end{pmatrix} = \frac{h_0^3}{(1+e_0\cos\theta)^2\sqrt{e_0^2+2e_0\cos\theta+1}}\begin{pmatrix} e_0+2\cos\theta \\ 2\sin\theta \\ -1 \end{pmatrix}. \tag{19}$$

Eq.s (**??**) can be best integrated by introducing the new variable $\tilde{E}$ which obeys:

$$\tan\frac{\tilde{E}}{2} = \sqrt{\frac{1-e_0}{1+e_0}}\tan\frac{\theta}{2}. \tag{20}$$

Note that $\tilde{E}$, although similar, does not correspond to the eccentric anomaly of the osculating orbit, except when $\theta = \theta_0$ at the beginning of the integration[3] . The following relations can be derived from Eq. (20):

$$\sin\theta = \frac{\sqrt{1-e_0^2}\sin\widetilde{E}}{1-e_0\cos\widetilde{E}},$$

$$\cos\theta = \frac{\cos\widetilde{E}-e_0}{1-e_0\cos\widetilde{E}},$$

$$\frac{d\widetilde{E}}{d\theta} = \frac{1-e_0\cos\widetilde{E}}{\sqrt{1-e_0^2}},$$

[3]In such case θ and e_0 concide with the true anomaly and eccentricity of the osculating orbit, respectively.

and substituted into Eqs. (19) yield:

$$\frac{dq_{11}}{d\widetilde{E}} = \frac{h_0^3}{(1-e_0^2)^2}\frac{e_0(e_0^2-2)\cos^2\widetilde{E}+2\cos\widetilde{E}-e_0}{\sqrt{1-e_0^2\cos^2\widetilde{E}}} \tag{21}$$

$$\frac{dq_{21}}{d\widetilde{E}} = \frac{h_0^3}{(1-e_0^2)^{3/2}}\frac{2\sin\widetilde{E}(1-e_0\cos\widetilde{E})}{\sqrt{1-e_0^2\cos^2\widetilde{E}}} \tag{22}$$

$$\frac{dq_{31}}{d\widetilde{E}} = \frac{-h_0^3}{(1-e_0^2)^2}\frac{(1-e_0\cos\widetilde{E})^2}{\sqrt{1-e_0^2\cos^2\widetilde{E}}} \tag{23}$$

Eq.s (21-23) can now be integrated. The full analytical solution, which for the cases of q_1 and q_3 involves elliptic integrals, are reported in Appendix I where series expansions are performed leading to the following compact form as a function of $\tilde{E}$:

$$q_{11}(h_0,e_0,\tilde{E}) = \frac{h_0^3}{(1-e_0)^2}\left[Q_{11}(e_0,\tilde{E})-Q_{11}(e_0,\tilde{E}_0)\right],$$

$$q_{21}(h_0,e_0,\tilde{E}) = \frac{h_0^3}{(1-e_0)^{3/2}}\left[Q_{21}(e_0,\tilde{E})-Q_{21}(e_0,\tilde{E}_0)\right],$$

$$q_{31}(h_0,e_0,\tilde{E}) = \frac{h_0^3}{(1-e_0)^2}\left[Q_{31}(e_0,\tilde{E})-Q_{31}(e_0,\tilde{E}_0)\right].$$

The analytical expressions for the functions $Q_i(e_0,\tilde{E})$ can be written as the sum of secular and oscillatory terms:

$$Q_{i1}(\tilde{E}) = Q_{i1,sec}(\tilde{E}) + Q_{i1,osc}(\tilde{E}).$$

The secular terms yield (see [6] for a complete derivation):

$$Q_{11,sec}(\tilde{E}) = k_1\tilde{E}$$

$$Q_{21,sec}(\tilde{E}) = 0$$

$$Q_{31,sec}(\tilde{E}) = k_3\tilde{E}$$

where k_1 and k_3 are given by:

$$k_1 = \frac{2\mathcal{E}(e_0)(2-e_0^2)-4\mathcal{K}(e_0)}{\pi e_0}$$

$$k_3 = \frac{2\mathcal{E}(e_0) - 4\mathcal{K}(e_0)}{\pi}$$

with $\mathcal{K}$ and $\mathcal{E}$ indicating complete elliptic integrals of the first and second kind, respectively:

$$\mathcal{K}(e_0) = \int_0^1 \frac{dz}{\sqrt{(1-z^2)(1-e_0^2z^2)}}$$

$$\mathcal{E}(e_0) = \int_0^1 \sqrt{\frac{1-e_0^2z^2}{1-z^2}}dz$$

The oscillatory terms are periodic functions of period 2π as[6]:

$$Q_{1,osc}(\tilde{E}) = (\mathcal{Q}_1 \boldsymbol{v}_{e0})^T \boldsymbol{v}_S$$

$$Q_{2,osc}(\tilde{E}) = (\mathcal{Q}_2 \boldsymbol{v}_{e0})^T \boldsymbol{v}_C$$

$$Q_{3,osc}(\tilde{E}) = (\mathcal{Q}_3 \boldsymbol{v}_{e0})^T \boldsymbol{v}_S$$

where:

$$\boldsymbol{v}_{e0} = \left(1, e_0, e_0^2, e_0^3 \ldots\right)^T$$

$$\boldsymbol{v}_S = \left(\sin\tilde{E}, \sin 2\tilde{E}, \sin 3\tilde{E}, \ldots\right)^T$$

$$\boldsymbol{v}_C = \left(\cos\tilde{E}, \cos 2\tilde{E}, \cos 3\tilde{E}, \ldots\right)^T$$

$$\mathcal{Q}_1 = \begin{bmatrix} 2 & 0 & 3/4 & 0 & 15/32 & \ldots \\ 0 & -1/2 & 0 & -1/8 & 0 & \ldots \\ 0 & 0 & 1/12 & 0 & 5/64 & \ldots \\ 0 & 0 & 0 & -1/32 & 0 & \ldots \\ 0 & 0 & 0 & 0 & 3/320 & \ldots \\ \vdots & \vdots & \vdots & \vdots & \vdots & \ddots \end{bmatrix}$$

$$\mathcal{Q}_2 = \begin{bmatrix} -2 & 0 & -1/4 & 0 & -3/32 & \ldots \\ 0 & 1/2 & 0 & 1/8 & 0 & \ldots \\ 0 & 0 & -1/12 & 0 & -3/64 & \ldots \\ 0 & 0 & 0 & 1/32 & 0 & \ldots \\ 0 & 0 & 0 & 0 & -3/320 & \ldots \\ \vdots & \vdots & \vdots & \vdots & \vdots & \ddots \end{bmatrix}$$

$$\mathcal{Q}_3 = \begin{bmatrix} 0 & 2 & 0 & 3/4 & 0 & \dots \\ 0 & 0 & -3/8 & 0 & -7/32 & \dots \\ 0 & 0 & 0 & 1/12 & 0 & \dots \\ 0 & 0 & 0 & 0 & -7/256 & \dots \\ 0 & 0 & 0 & 0 & 0 & \dots \\ \vdots & \vdots & \vdots & \vdots & \vdots & \ddots \end{bmatrix}$$

Second order terms, whose derivation is dealt with in [6], are here omitted.

The radial position as well as the orbit eccentricity, semimajor axis and angular momentum can be derived through Eq.s (11,4,7,6).

3.1 Time of Flight

So far we have obtained the orbit characteristics as a function of the variables $\tilde{E}$ and θ. The last step is now to obtain the generalized orbital elements as a function of time so that the spacecraft position and velocity can be inferred at any given epoch.

The time t corresponding to a given θ for the perturbed trajectory can be conveniently written as a series expansion:

$$t(\epsilon, \theta) = t_0(\theta) + \epsilon t_1(\theta) + o(\epsilon) \tag{24}$$

where $t_0(\theta)$ correspond to the time of the unperturbed trajectory and the remaining part is the thrust-induced *phasing difference* between the perturbed and unperturbed trajectory:

$$\Delta t(\epsilon, \theta) = \epsilon t_1(\theta) + o(\epsilon)$$

By substituting Eq.(24) into Eq.(9) we obtain:

$$\frac{dt}{d\theta} = \frac{dt_0}{d\theta} + \epsilon \frac{dt_1}{d\theta} = \frac{1}{q_3 s^2} \tag{25}$$

After substituting the expansions (15) into Eq.(25), expanding in Taylor series and collecting terms of equal power of epsilon we obtain:

$$\frac{dt_1}{d\theta} = -\frac{q_{31}}{q_{30} s_0^3}(s_0 + 2q_{30}) - \frac{2q_{11}}{q_{30} s_0^3}\cos\theta - \frac{2q_{12}}{q_{30} s_0^3}\sin\theta \tag{26}$$

where:

$$s_0 = q_{10}\cos\theta + q_{30} = q_{30}(1 + e_0\cos\theta).$$

Eq.(26) can be conveniently written with respect to the variable $\tilde{E}$ as:

$$\begin{aligned} \tfrac{dt_1}{d\tilde{E}} = {} & \tfrac{3e_0 - (2+2e_0^2)\cos\tilde{E} + e_0\cos 2\tilde{E}}{q_{30}^4(1-e_0^2)^{5/2}} q_{11}(\widetilde{E}) - \tfrac{2\sin\tilde{E} - e_0\sin 2\tilde{E}}{q_{30}^4(1-e_0^2)^2} q_{21}(\tilde{E}) + \\ & - \tfrac{3-(5e_0-e_0^3)\cos\tilde{E} + e_0^2\cos 2\tilde{E}}{q_{30}^4(1-e_0^2)^{5/2}} q_{31}(\tilde{E}) \end{aligned} \tag{27}$$

The integration process is performed in [6] leading to the following compact form:

$$\Delta t(e_0,\theta) = \frac{\epsilon h_0^7}{(1-e_0)^{9/2}} \left[T(\tilde{E}) - T(\tilde{E}_0)\right],$$

where the function $T(\tilde{E})$ can be written as:

$$T(\widetilde{E}) = T_{sec}(\widetilde{E}) + T_{osc}(\widetilde{E}).$$

The *secular* part yields:

$$T_{sec}(\tilde{E}) = \tfrac{3}{2}(k_1 e_0 - k_3)\,\tilde{E}^2 + \tilde{E}\left[\left(k_3 e_0(5-e_0^2) - 2k_1(1+e_0^2)\right)\sin\tilde{E} + \right.$$
$$\left. + \tfrac{1}{2} e_0 (k_1 - k_3 e_0)\sin 2\tilde{E} + g(e_0,\tilde{E}_0)\right]$$

where:

$$g(e_0,\tilde{E}_0) = \left(\boldsymbol{G}\boldsymbol{v}_{e0}\right)^T \boldsymbol{w}_{S0}$$

with:

$$\boldsymbol{w}_{S0} = \left(1, \sin\tilde{E}_0, \sin 2\tilde{E}_0, \sin 3\tilde{E}_0, \ldots\right)^T,$$

and

$$\boldsymbol{G} = \begin{bmatrix} 3k_3\tilde{E}_0 & -3k_1\tilde{E}_0 & 0 & 0 & 0 & \ldots \\ 0 & 0 & 0 & 0 & 0 & \ldots \\ 0 & 0 & 3/8 & 0 & -9/32 & \ldots \\ 0 & 0 & 0 & 0 & 0 & \ldots \\ 0 & 0 & 0 & 0 & 3/256 & \ldots \\ \vdots & \vdots & \vdots & \vdots & \vdots & \ddots \end{bmatrix}$$

Finally, the *oscillatory* part yields:

$$T_{,osc}(\tilde{E}) = \left(\boldsymbol{H}\boldsymbol{v}_{e0}\right)^T \boldsymbol{v}_C + p_1\cos\tilde{E} + p_2\sin\tilde{E} + p_3\cos 2\tilde{E} + p_4\sin 2\tilde{E}$$

where:

$$\boldsymbol{H} = \begin{bmatrix} 4-2k_1 & 5k_3 & -2k_1-10/3 & -k_3-5/24 & -11/30 \\ 0 & k_1/4-1 & -k_3/4+13/48 & 5/6 & -17/192 \\ 0 & 0 & 0 & -1/8 & 0 \\ 0 & 0 & 0 & 0 & 317/15360 \\ 0 & 0 & 0 & 0 & 0 \end{bmatrix}$$

and

$$p_1 = \left(\boldsymbol{P}_1\boldsymbol{v}_{e0}\right)^T \boldsymbol{v}_{C0}$$

$$p_2 = \left(\boldsymbol{P}_2 \boldsymbol{v}_{e0}\right)^T \boldsymbol{v}_{S0}$$

$$p_3 = \left(\boldsymbol{P}_3 \boldsymbol{v}_{e0}\right)^T \boldsymbol{v}_{C0}$$

$$p_4 = \left(\boldsymbol{P}_4 \boldsymbol{v}_{e0}\right)^T \boldsymbol{v}_{S0}$$

with

$$\boldsymbol{P}_1 = \begin{bmatrix} -4 & 1 & 10/3 & -\frac{11}{16} & \frac{11}{30} & -\frac{5}{16} \\ 4 & 0 & -7/2 & 0 & -\frac{5}{16} & 0 \\ 0 & -1 & 0 & 3/4 & 0 & 1/4 \\ 0 & 0 & 1/6 & 0 & -\frac{7}{96} & 0 \\ 0 & 0 & 0 & -1/16 & 0 & 1/16 \\ 0 & 0 & 0 & 0 & \frac{3}{160} & 0 \end{bmatrix}$$

$$\boldsymbol{P}_2 = \begin{bmatrix} 2k_1\tilde{E}_0 & -5k_3\tilde{E}_0 & 2k_1\tilde{E}_0 & k_3\tilde{E}_0 & 0 & 0 \\ 4 & 0 & -9/2 & 0 & \frac{11}{16} & 0 \\ 0 & -1 & 0 & 5/8 & 0 & \frac{15}{32} \\ 0 & 0 & 1/6 & 0 & -\frac{3}{32} & 0 \\ 0 & 0 & 0 & -1/16 & 0 & \frac{19}{256} \\ 0 & 0 & 0 & 0 & \frac{3}{160} & 0 \end{bmatrix}$$

$$\boldsymbol{P}_3 = \begin{bmatrix} 0 & 1 & -1/4 & -5/6 & \frac{11}{64} & -\frac{11}{120} \\ 0 & -1 & 0 & \frac{7}{8} & 0 & \frac{5}{64} \\ 0 & 0 & 1/4 & 0 & -3/16 & 0 \\ 0 & 0 & 0 & -1/24 & 0 & \frac{7}{384} \\ 0 & 0 & 0 & 0 & \frac{1}{64} & 0 \\ 0 & 0 & 0 & 0 & 0 & -\frac{3}{640} \end{bmatrix}$$

$$\boldsymbol{P}_4 = \begin{bmatrix} 0 & -\frac{k_1\tilde{E}_0}{2} & \frac{k_3\tilde{E}_0}{2} & 0 & 0 & 0 \\ 0 & -1 & 0 & 5/8 & 0 & \frac{9}{64} \\ 0 & 0 & 1/4 & 0 & -1/8 & 0 \\ 0 & 0 & 0 & -1/24 & 0 & \frac{1}{384} \\ 0 & 0 & 0 & 0 & \frac{1}{64} & 0 \\ 0 & 0 & 0 & 0 & 0 & -\frac{3}{640} \end{bmatrix}$$

Finally, the zeroth order (i.e. unperturbed) part of the time function obeys Kepler's equation:

$$t_0(\tilde{E}) = \frac{h_0^3}{(1-e_0^2)^{3/2}} \left[T_{kep}(\tilde{E}) - T_{kep}(\tilde{E}_0) \right],$$

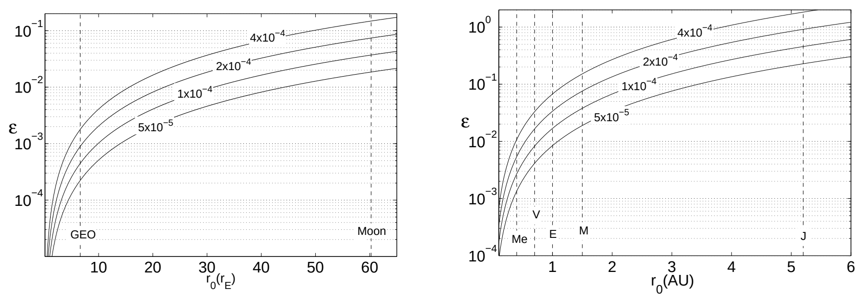

Figure 1: Variability of the parameter epsilon for Earth (right) and interplanetary orbits (left)

where:

$$T_{kep}(\tilde{E}) = \tilde{E} - e_0 \sin \tilde{E}.$$

3.1 Variability of the Parameter ϵ

The variability of the parameter ϵ for Earth and interplanetary orbits is plotted in Fig (1) considering different values of the tangential accelerations ranging from 50 to 400 mN/tonne. In general the parameter ϵ is much smaller in Earth orbit than in interplanetary space, meaning that interplanetary orbits are more difficult to propagate analytically. Low thrust orbit transfer beyond Mars with tangential acceleration exceeding 100 mN/tonne would in general be difficult to reproduce with the current analytical solution. Yet, due to the rapid decrease of the available solar energy, such case would imply the use of nuclear electric propulsion, a space technology which has not yet been developed. On the other hand, when considering trajectories to the inner planets the higher value of the local solar gravity helps reducing ϵ so that accurate analytical propagations can be obtained. An example of low thrust interplanetary transfer to Mercury is reported later on.

4 Propagation

By comparison with an accurate numerical solution one can see that as long as the parameter epsilon remains small the above formulas represent fairly accurately the system dynamics along at least one revolution. Depending on the value of ϵ, for the multiple-revolution case, the accuracy of the analytical representation will start to deteriorate for large θ and this will occur the earlier the larger ϵ. In order to overcome this limitation the analytical expressions needs to be updated along the trajectory by referring each time to an updated value of the dimensionless angular momentum h_0 and eccentricity e_0. When doing this a complication arises due to the fact that, in general, the osculating ellipse at the update point has undergone a precession of its apses line which makes the new initial value of the q_2 orbital parameter (Eq. (2)) different from zero. Yet the previously derived analytical formulas for the evolution of q_1, q_2, q_3, are based on the fact that $q_{20} = 0$ which greatly simplifies the analytical integration process. To overcome this difficulty a change of variable is performed which allows to keep using the previous formulas. The procedure is described in the following.

Let us suppose that at the angular position $\hat{\theta}$ we want to reset the propagation. The starting orbit will be characterized by a new value of the eccentricity, $\hat{e}$, angular momentum $\hat{h}$, and eccentricity vector rotation $\hat{\Delta\gamma}$. We then introduce the new variables:

$$\theta' = \theta - \hat{\Delta\gamma} \tag{28}$$

$$\Delta\gamma' = \Delta\gamma - \hat{\Delta\gamma} \tag{29}$$

$$q_1' = \frac{e}{h}\cos\Delta\gamma' \tag{30}$$

$$q_2' = \frac{e}{h}\sin\Delta\gamma' \tag{31}$$

$$q_3' = 1/h \tag{32}$$

At the beginning of the new propagation step, that is when the value of θ' is given by:

$$\theta_0' = \hat{\theta} - \hat{\Delta\gamma},$$

we have:

$$\Delta\gamma' = \Delta\gamma(\theta = \hat{\theta}) - \hat{\Delta\gamma} = 0,$$

so that the initial value for the new generalized orbital elements has the same structure as found in Eq.s (16-18):

$$q_1'(\theta_0') = \frac{\hat{e}}{\hat{h}}, \tag{33}$$

$$q_2'(\theta_0') = 0, \tag{34}$$

$$q_3'(\theta_0') = \frac{1}{\hat{h}}, \tag{35}$$

and the q_i' can be propagated with the previously derived formulas to yield:

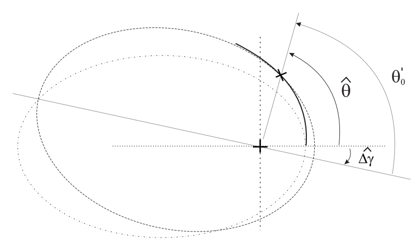

Figure 2: Schematic of analytical propagation. The instantaneous trajectory is denoted with a solid line. The dash-dot line ellipse represents the initial osculating orbit which is propagated analytically up to $\theta = \hat{\theta}$ where the new osculating orbit is the dash line ellipse. A change of variable (Eq.s (28-32)) is necessary to compensate for the accumulated apses line rotation $\hat{\Delta\gamma}$.

$$q_1' = \frac{\hat{e}}{\hat{h}} + \frac{\epsilon \hat{h}^3}{(1-\hat{e}^2)^2}\left[Q_{11}(\hat{e},\theta') - Q_{11}(\hat{e},\theta_0')\right],$$

$$q_2' = \frac{\epsilon \hat{h}^3}{(1-\hat{e}^2)^{3/2}}\left[Q_2(\hat{e},\theta') - Q_2(\hat{e},\theta_0')\right],$$

$$q_3' = \frac{1}{\hat{h}} + \frac{\epsilon \hat{h}^3}{(1-\hat{e}^2)^2}\left[Q_3(\hat{e},\theta') - Q_3(\hat{e},\theta_0')\right].$$

Finally, we can transfer back to the main variable $q_1, ..., q_3$ using the rotation:

$$\begin{pmatrix} q_1(\theta) \\ q_2(\theta) \\ q_3(\theta) \end{pmatrix} = \begin{bmatrix} \cos\hat{\Delta\gamma} & -\sin\hat{\Delta\gamma} & 0 \\ \sin\hat{\Delta\gamma} & \cos\hat{\Delta\gamma} & 0 \\ 0 & 0 & 1 \end{bmatrix} \begin{pmatrix} q_1'(\theta - \hat{\Delta\gamma}) \\ q_2'(\theta - \hat{\Delta\gamma}) \\ q_3'(\theta - \hat{\Delta\gamma}) \end{pmatrix},$$

which follows from Eq.s (29-32).

For weakly perturbed orbits (say $\epsilon < 1 \times 10^{-2}$) sufficient accuracy can be obtained with one update per revolution. By performing the update a few times per revolution it will then be possible to achieve high accuracy even for higher value of the parameter epsilon (say $\epsilon < 1 \times 10^{-1}$). As the value of ϵ becomes excessively high, the number of required update points will make the analytical method more similar to a numerical propation scheme hence diminishing its appeal.

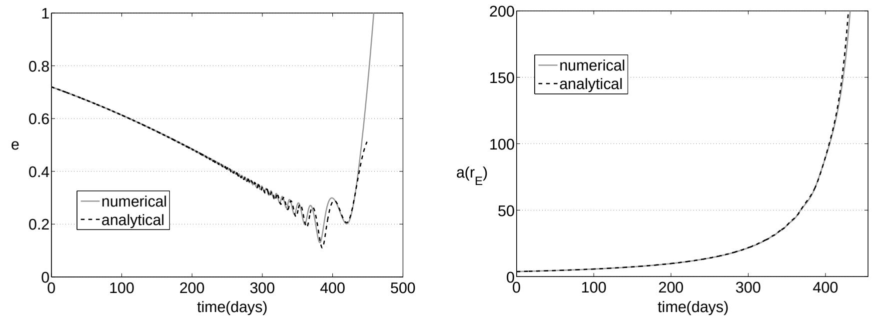

Figure 3: Comparison between analytical and numerical solution for an orbit raising maneuver from GTO to earth escape. Plotted quantities are the orbit eccentricity (left) and semimajor axis (right). The analytical formulas are propagated once per orbital revolution.

5 Results

Simulations have been run to compare the analytical formulas with an accurate numerical integration. We have considered two test cases: an orbit transfer from a geostationary transfer orbit to Earth escape and an interplanetary low-thrust trajectory from Earth to Mercury.

5.1 GTO to Earth escape

For the first test case we consider a spacecraft in a earth geostationary transfer orbit of eccentricity e_0=0.72 and initial semimajor axis of 24000 km, subject to a continuous and constant tangential acceleration A_t=100 mN/tonne and neglecting other perturbative accelerations[4]. Assuming the orbit transfer starts at pericenter the corresponding dimensionless angular momentum is $h_0 = \sqrt{1+e_0} \approx 1.3$ while the dimensionless tangential acceleration is $\epsilon = A_t/g_0 \approx 1.13 \times 10^{-5}$,where $g_0 \approx 8.28\ m/s^2$ is the local gravitational acceleration at the beginning of the orbit raising maneuver. The comparison between analytical and numerical solution is plotted in Fig. 3. Given the small value of epsilon a very accurate analytical solution up to almost orbit escape is obtained by propagating the analytical formulas once per orbital revolution.

5.1 Earth to Mercury

For the second test case we consider a 35-months low-thrust orbit transfer from Earth to Mercury employing a constant and continuous thrust A_t=200

[4]the same example is reported on page 249 of reference[8]

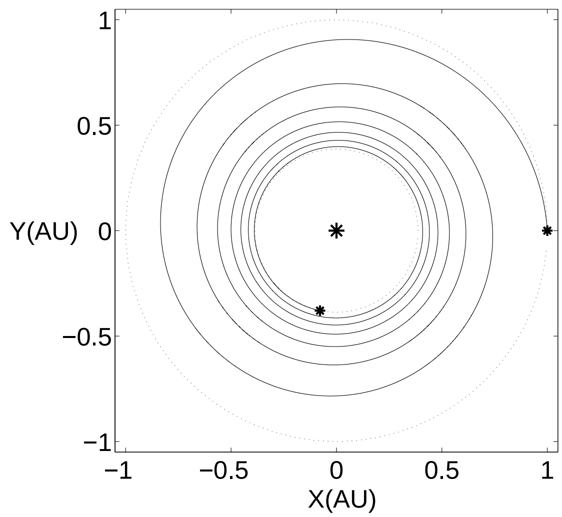

Figure 4: Low thrust Earth-Mercury orbit transfer. Planets orbits are assumed coplanar and circular for simplicity. The small difference between the numerical and analytical trajectory cannot be appreciated from this plot.

mN/tonne. For simplicity the Earth and Mercury orbits are considered colpanar and circular. A launch ΔV of 2 km/s in the inward radial direction is applied to the spacecraft in order to arrive at Mercury with almost zero relative velocity. This results in an initial eccentricity $e_0 \simeq$0.067 while the initial dimensionless angular momentum is $h_0 = 1$. The dimensionless tangential acceleration is $\epsilon = A_t/g_0 \approx -3.37 \times 10^{-2}$,where $g_0 \approx 0.0059$ m/s^2 is the sun gravitational acceleration at 1 AU. The interplanetary trajectory is depicted in Figure 4 while a comparison between numerical and analytical solution is presented in Figure 5. Due to the much higher value of epsilon, compared with the previous case, the analytical formulas have been propagated 8 times per revolution in order to achieve sufficient accuracy. It is interesting to point out that, compared with a high accuracy orbit propagator, the analytical methods provides an error at Mercury encounter of 0.0223 AU.

Note that in a a real mission scenario the need to perform a plane change maneuver severly complicates the trajectory design problem introducing thrust arcs with time-varying in- and out-of-plane thrust components. While the current model is clearly not suitable to describe these types of trajectories an attempt to extend its capability to the three-dimensional case will be conducted in the future.

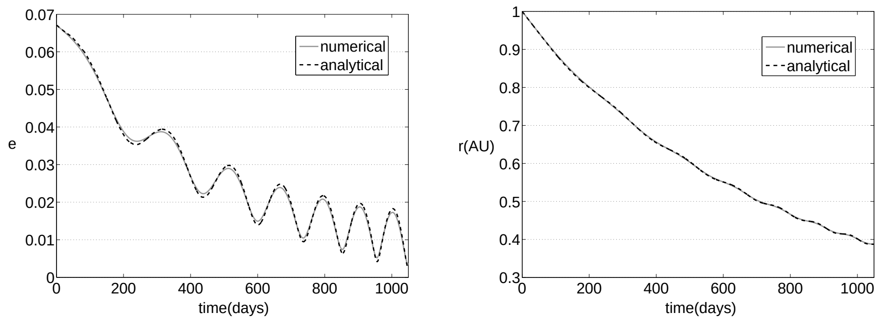

Figure 5: Comparison between analytical and numerical solution for an orbit raising maneuver from GTO to earth escape. The analytical formulas are here propagated eigth times per orbital revolution

5 Conclusions

A new asymptotic solution for the two-body problem perturbed by constant tangential acceleration has been provided with the aid of a special perturbation formulation of the orbit equations of motion. Relatively compact analytical formulas accurately represent the trajectory evolution in time accounting for both secular and oscillatory variations of the orbital elements and ar not limited by high values of the orbit eccentricity. The accuracy of the method has been tested with highly eccentric Earth orbits evolving beyond lunar distance and interplanetary orbits to the inner solar system planets referring to tangential acceleration magnitude achievable by state-of-the-art electric propulsion engines. It is seen that for small values (say $\epsilon < 1 \times 10^{-4}$) of the non-dimensional acceleration magnitude, as it is the case in Low Earth Orbit, the approximate analytical solution can be used to accurately represent the orbit evolution along very large intervals without iterating the process. For the worse case scenario in which the acceleration magnitude is high compared to local gravity, which is the case of interplanetary orbits, high accuracy can be retained by updating the values of the initial generalized parameters a few times along each orbit.

Future work will address the more general problem in which the tangential acceleration is not constant along the orbit and the extension of the method to non-planar trajectories.

5 Acknowledgements

The work for this paper was supported by the project “Propagation of Orbits, Advanced Orbital Dynamics and Use of Space Tethers” supported by the Dirección General de Investigación (DGI) of the Spanish Ministry of Education and Science through the contract ESP2007-64068.

References

[1] D. Benney, "Escape from a circular orbit using tangential thrust," *Jet Propulsion*, vol. 28, no. 3, pp. 167–169, 1958.

[2] F. Boltz, "Orbital motion under continuous tangential thrust," *Journal of Guidance Control Dynamics*, vol. 15, pp. 1503–1507, 1992.

[3] R. H. Battin, *An introduction to the mathematics and methods of astrodynamics.* AIAA, 1999.

[4] J. Kechichian, "Orbit raising with low-thrust tangential acceleration in presence of earth shadow," *Journal of Spacecraft and Rockets*, vol. 35, no. 4, 1998.

[5] Y. Gao and C. Kluever, "Analytic orbital averaging technique for computing tangential-thrust trajectories," *Journal of Guidance, Control, and Dynamics*, vol. 28, no. 6, pp. 1320–1323, 2005.

[6] C. Bombardelli and J. Pelaez, "Asymptotic Solution for the Two-Body Problem with Constant Tangential Acceleration." Celestial Mechanics and Dynamical Astronomy. Submitted for publication.

[7] J. Pelaez, J. Hedo, and P. de Andres, "A special perturbation method in orbital dynamics," *Celestial Mechanics and Dynamical Astronomy*, vol. 97, no. 2, pp. 131–150, 2007.

[8] S. Kemble, "Interplanetary mission analysis and design," 2006.